

# Analytical model of the Ultrabroadband Operation of Transverse-Coupled-Cavity VCSELs

Valerio Torrelli<sup>\*†</sup>, Martino D'Alessandro<sup>\*†</sup>, Lorenzo Miri<sup>\*</sup>, Pierluigi Debernardi<sup>†</sup>,  
Francesco Bertazzi<sup>\*†</sup>, Michele Goano<sup>\*†</sup>, Mariangela Gioannini<sup>\*</sup>, Alberto Tibaldi<sup>\*†</sup>

<sup>\*</sup> Dipartimento di Elettronica e Telecomunicazioni, Politecnico di Torino, Corso Duca degli Abruzzi 24, 10129 Torino, Italy

<sup>†</sup> CNR-IEIIT, Corso Duca degli Abruzzi 24, 10129 Torino, Italy

E-mail: martino.dalessandro@polito.it

**Abstract**—The ultrabroadband operation of transverse-coupled-cavity vertical-cavity-surface-emitting lasers is investigated in this work. Relying on a closed-form expression of the intensity modulation response, our model allows for an extended and fast parametric campaign of the design inputs, as well as an easy interpretation of the bandwidth enhancement.

## I. INTRODUCTION

High-speed intradatecenter low-loss communications have become essential in today's rapidly advancing digital landscape. To this end, innovative technologies have been explored, one of which is represented by transverse coupled cavity (TCC) vertical-cavity surface-emitting lasers (VCSELs) [1]. In this work we investigate the ultrabroadband operation of these devices by means of delayed rate equation models [2]–[5]. Under weak feedback conditions [3], [6] and only counting one round trip, such systems can be reduced to the famous Lang-Kobayashi model [7]. Instead of solving these delayed differential equations (DDE) numerically, here we derive a closed-form expression for the corresponding small signal system, yielding an analytical intensity modulation (IM) response. The analytical nature of our model allows for an extensive parametric campaign, as well as an easy interpretation of the bandwidth enhancement phenomenon, paving the way towards further optimizations.

## II. DESCRIPTION OF THE MODEL

The starting point is the system of DDE and the geometry provided in [3] and sketched in Fig. 1. It consists of a VCSEL laterally coupled with  $M$  cavities (indexed by the subscript  $m$ ) characterized by an absorption coefficient  $\alpha_{C,m}$ , propagation constant  $\beta_{C,m}$ , group velocity  $v_{g,m}$ , cavity length  $L_{C,m}$  and its corresponding round trip delay  $\tau_m$ . Furthermore  $\eta_m \in [0, 1]$  quantifies the coupling strength for each cavity. In these rate equations, each reflection in the transverse coupled cavities is viewed as a delayed term in the photon equation. This assumption comes from a multiple-reflection interpretation of the transverse resonance condition. The model, including  $P$  reflections indexed by the subscript  $p$ , reads:

$$\begin{cases} \partial_t N + AN + BN^2 + CN^3 + G_d v_g (N - N_{tr}) (1 - \epsilon S) S - \frac{I}{qAd_{AR}} = 0 \\ \partial_t S - [\Gamma G_d v_g (N - N_{tr}) (1 - \epsilon S) - \mathcal{L}] S - \Gamma \beta_{sp} B N^2 = 0, \end{cases} \quad (1)$$

where  $N$  and  $S$  represent the carrier and photon densities

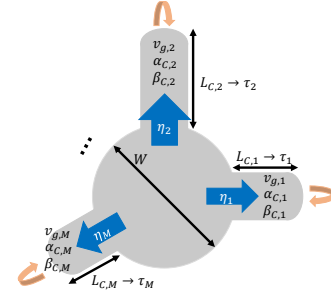


Fig. 1. Schematics of a TCC-VCSEL section.

and  $\mathcal{L}$  represents the losses. The other symbols have the same meaning as in [2], [3], [8]. Losses are expressed as:

$$\mathcal{L} = \frac{1}{\tau_p} - \sum_{m=1}^M \frac{v_{g,m}}{W} \log |U_m|, \quad (2)$$

with:

$$U_m = 1 + \frac{\eta_m}{1 - \eta_m} \sum_{p=1}^P \left( \sqrt{1 - \eta_m} \right)^p \cdot e^{-2p\alpha_{C,m} L_{C,m}} e^{-j2p\beta_{C,m} L_{C,m}} \sqrt{\frac{S(t - p\tau_m)}{S(t)}} \quad (3)$$

which accounts for the multiple reflections. (2) suggests that the equivalent losses  $\mathcal{L}$  depend on the past-to-present photon density ratios, *i.e.*,  $r_{m,p} \triangleq S(t - p\tau_m) / S(t)$ , so that  $\mathcal{L}$  is a function of  $M \times P$  variables. At steady state the densities are constant, yielding  $r_{m,p} = 1$ . If a small signal is applied on top of a bias,  $r_{m,p}$  exhibits small variations around 1, thus it is possible to perform a first order Taylor expansion of  $\mathcal{L}$  like:

$$\mathcal{L} \simeq \mathcal{L}^{(0)} + \sum_{m,p} \mathcal{L}'_{m,p} (r_{m,p} - 1), \quad (4)$$

where  $\mathcal{L}^{(0)} \triangleq \mathcal{L} \Big|_{r_{m,p}=1}$  and  $\mathcal{L}'_{m,p} \triangleq \frac{\partial \mathcal{L}}{\partial r_{m,p}} \Big|_{r_{m,p}=1}$ .  $\mathcal{L}^{(0)}$  indicates the steady-state threshold losses. In this model the photon lifetime  $\tau_p$  is given as an input ensuring  $\mathcal{L}^{(0)} > 0$ . Inserting (4) into (1) and regrouping the steady state terms into  $R_N(N, S)$  and  $R_S(N, S)$ , the system can be rewritten as:

$$\begin{cases} \partial_t N + R_N(N, S) = 0 \\ \partial_t S + R_S(N, S) + \sum_{m,p} \mathcal{L}'_{m,p} (r_{m,p} - 1) = 0. \end{cases} \quad (5)$$

Exploiting again the small signal condition, let us define the unknowns as the sum of the DC component and the small variation around it:  $N \rightarrow N_0 + \delta N$ ,  $S \rightarrow S_0 + \delta S$  and  $I \rightarrow I_0 + \delta I$ . Assuming a time-harmonic dependency  $e^{-j\omega t}$ , the time derivative operator becomes  $-j\omega$  and the time shift operator of  $p\tau_m$  becomes  $e^{j\omega p\tau_m}$ . The overall system becomes:

$$\begin{bmatrix} \underline{J}_{=0} + \underline{J}_1(\omega) + \underline{J}_F(\omega) \\ \delta N \\ \delta S \end{bmatrix} = \begin{bmatrix} \delta I / (qAd_{AR}) \\ 0 \end{bmatrix}, \quad (6)$$

where  $\underline{J}_{=0}$  is the Jacobian matrix of the steady-state system evaluated at the bias point, *i.e.*,

$$\underline{J}_{=0} = \begin{bmatrix} \partial_N R_N & \partial_S R_N \\ \partial_N R_S & \partial_S R_S \end{bmatrix}, \quad (7)$$

$\underline{J}_1 = -j\omega \underline{I}$ , where  $\underline{I}$  is the identity matrix and

$$\underline{J}_F = \begin{bmatrix} 0 & 0 \\ 0 & \sum_{m,p} \mathcal{L}'_{m,p} (e^{j\omega p\tau_m} - 1) \end{bmatrix}, \quad (8)$$

where the feedback losses are defined as  $\mathcal{F}(\omega) \triangleq \sum_{m,p} \mathcal{L}'_{m,p} (e^{j\omega p\tau_m} - 1)$ . Please note that the solution of (6) can be found analytically. Furthermore, in order to find the minima of the modulus of the determinant of (6), one should solve a transcendental equation. These correspond to the resonant frequencies [8].

### III. RESULTS AND DISCUSSION

A figure of merit of high-speed lasers is the frequency  $f_{3dB}$  at which their IM response intersects the  $-3$  dB level, namely the cutoff frequency.

$f_{3dB}$  is analysed as a function of the coupling strength  $\eta$  and the cavity number  $M$  in Fig. 2, assuming equal cavities. The optimal value of  $\eta$  decreases for an increasing number of cavities, which is in agreement with [3]. As an additional validation, our linearized model was also compared with the numerical DDE solution [9] of (1) (black dashed lines in Fig. 3).

Finally, in Fig. 3 the intensity modulation of a device with 5 cavities with the same  $L_C = 6.9 \mu\text{m}$  and different coupling strengths is reported. As expected from Fig. 2, the strongly coupled case is worse than the weakly coupled one. In addition, the weakly coupled case also exhibits a photon-photon resonance peak above cut-off.

To interpret the bandwidth enhancement, it can be noted from (6) that, if  $\underline{J}_F(2, 2) = -\underline{J}_1(2, 2)$ , *i.e.*,  $\mathcal{F}(\omega) = +j\omega$ , the time-derivative term in the photon rate equation gets

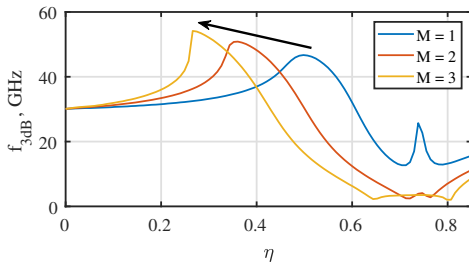


Fig. 2. Cutoff frequency against the coupling strength  $\eta$  for a different number of coupled cavities ( $L_C = 6.9 \mu\text{m}$ ).

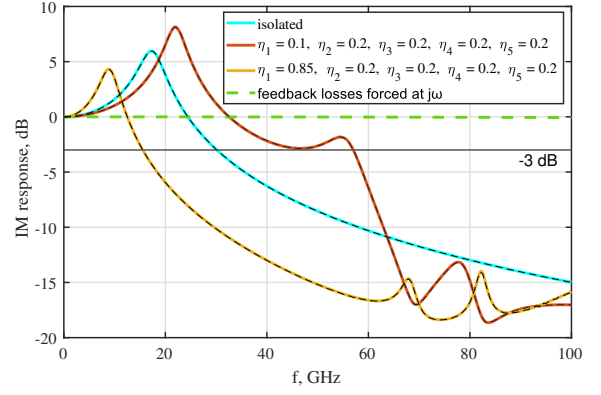


Fig. 3. Photon response of different cases. Ideal response  $\mathcal{F}(\omega) = j\omega$  (green); isolated cavity case (cyan); TCC with 5 weakly coupled cavities (red); TCC with one of the 5 cavities strongly coupled (yellow). The dashed black lines are the DDE numerical solutions [9] of (1), validating our linearization.

compensated by the feedback term. In this case the overall dynamic behaviour is only determined by the carrier equation, leading to an extremely high  $f_{3dB}$ . In Fig. 3 we forced the feedback term at the ideal value of  $j\omega$ , obtaining the dashed green line, which is flat over the investigated frequency range.

### IV. CONCLUSIONS

In this work, we investigated the ultrabroadband operation of TCC-VCSELs by means of a linearized delayed rate equation model, obtaining a closed form for the small signal system which allows to perform an extended parametric campaign in a much faster way with respect to the numerical DDE approach. Furthermore, the analytical formulation allows not only for an easy interpretation of the mechanism underlying the bandwidth enhancement, but sets a design target:  $\mathcal{F}(\omega)$  as close as possible to  $j\omega$  for a large range of frequencies.

### ACKNOWLEDGMENT

This work was partially supported by the European Union – Next Generation EU under the Italian National Recovery and Resilience Plan (PNRR M4C2, Investimento 1.4 - Avviso n. 3138 del 16/12/2021 - CN00000013 National Centre for HPC, Big Data and Quantum Computing (HPC) - CUP E13C22000990001), by the photonics technology center PhotoNext@PoliTO and by Cisco Systems, Inc., under the Sponsored Research Agreement MULTI-VCSEL.

### REFERENCES

- [1] M. Lindemann, *et al.*, *2023 23rd International Conference on Transparent Optical Networks (ICTON)* (IEEE, 2023).
- [2] M. Ahmed, A. Bakry, M. S. Alghamdi, H. Dalir, F. Koyama, *Optics Express* **23**, 15365 (2015).
- [3] E. Heidari, *et al.*, *Nanophotonics* **10**, 3779 (2021).
- [4] M. Ahmed, *Applied Physics B* **126**, 170 (2020).
- [5] M. Ahmed, A. Bakry, *Pramana* **95**, 88 (2021).
- [6] H. Dalir, F. Koyama, *IEICE Electronics Express* **8**, 1075 (2011).
- [7] R. Lang, K. Kobayashi, *IEEE journal of Quantum Electronics* **16**, 347 (1980).
- [8] L. A. Coldren, S. W. Corzine, M. L. Mashanovitch, *Diode lasers and photonic integrated circuits* (John Wiley & Sons, 2012).
- [9] L. F. Shampine, S. Thompson, *Applied Numerical Mathematics* **37**, 441 (2001).